Journal of Colloid and Interface Science 329 (2009) 89–96

Contents lists available at ScienceDirect

Journal of Colloid and Interface Science

www.elsevier.com/locate/jcis

Precipitation of different calcite crystal morphologies in the presence of sodium stearate

Marko Ukrainczyk, Jasminka Kontrec, Damir Kralj *

Laboratory for Precipitation Processes, Ruđer Bošković Institute, Bijenička cesta 54, PO Box 180, HR-10002 Zagreb, Croatia

ARTICLE INFO

Article history:
Received 18 June 2008
Accepted 12 September 2008
Available online 23 September 2008

Keywords:
Precipitated calcium carbonate (PCC)
Calcite
Carbonation
Adsorption
Stearate
Hydrophobicity

ABSTRACT

The influence of sodium stearate (NaSt) on the precipitation of calcium carbonate during the semicontinuous process of slaked lime carbonation was studied in the systems in which process parameters, like concentration of total dissolved calcium, temperature, CO_2 flow rate and initial addition rate of slaked lime, were controlled. It was found that calcite was the only calcium carbonate polymorph that appeared under the investigated experimental conditions, while FT-IR spectroscopy and thermogravimetric analysis of samples confirmed the presence of stearate on the surface of precipitated calcium carbonate (PCC). Specific surface area of PCC increased with increasing stearate content: the highest value, $s = 52.8\ \mathrm{m^2\,g^{-1}}$, was obtained at $t = 20\,^\circ\mathrm{C}$, $c_\mathrm{tot} = 17.0\ \mathrm{mmol\,dm^{-3}}$ and the stearate content of $m_\mathrm{NaSt}/m_\mathrm{CaO} = 0.03$. It was also found that hydrophobic calcite crystals in the form of rhombohedral and scalenohedral morphology can be produced at $m_\mathrm{NaSt}/m_\mathrm{CaO} > 0.01$. The exception is the case of nanosized PCC production, when much higher concentration of NaSt is needed, $m_\mathrm{NaSt}/m_\mathrm{CaO} = 0.22$. Minimal amount of stearate necessary to build up the monolayer and corresponding cross sectional area of one stearate molecule were estimated for the obtained calcite morphologies.

1. Introduction

Precipitated calcium carbonate (PCC) is synthetic product, which has found large application in various fields of industry, mainly as filler and/or pigment. Introduction of new technologies, caused by the market demands for the high quality products, requires from PCC different physical and chemical properties. For example, final properties of the polymer/PCC composites depend strongly on the morphology, size distribution, surface characteristics and degree of dispersion of the PCC filler. Dispersion of the filler particles in the polymer matrix is of great importance, especially when using PCC of high specific surface area with tendency to agglomerate. However, the incompatibility of PCC hydrophilic surface with the hydrophobic polymers is a particular problem. Therefore, the surface of calcite is often modified by a variety of surfactants, among which fatty acids, or one of their salts, are most commonly used [1–5]. As a result, a hydrophobic alkyl chains is chemisorbed to the mineral surface, thus affecting the surface forces between the filler and the polymer matrix. On the other hand, the knowledge on the minimum quantity of fatty acid molecules that could produce the hydrophobic precipitate suitable for use as filler in polymer materials is of importance, because the excess of surfactant could deteriorate the physical chemical properties of composite.

The most widely used method of PCC production at industrial scale is the so-called carbonation route, comprising a batch process of CO_2 bubbling through an aqueous $Ca(OH)_2$ suspension. The principle disadvantage of batch carbonation of slaked lime is limited possibility of controlling the supersaturation of the system [6,7]. However, bench scale investigations have shown that an additional control of the morphology and size of precipitated particles is possible by running carbonation as a semicontinuous process [6,8]. It was also shown that calcite crystals, having different morphologies (rhombohedral, truncated prismatic, scalenohedral, spheroidal or chain-like agglomerates), could be produced by varying a range of process parameters during the process of semicontinuous carbonation, like temperature, concentration of total dissolved calcium, CO_2 flow rate, mass concentration of $Ca(OH)_2$ and addition rate of $Ca(OH)_2$ [9].

Keum et al. prepared hydrophobic composite particles of $CaCO_3$ directly by crystallization via solution route with a sodium trisilanolate [10,11], rather then modifying the resultant PCC products. Recently, hydrophobic PCC was also directly obtained by the batch carbonation process [12–14]. The best results of the surface modification were obtained when sodium oleate was added at the hydrating stage of quicklime [15]. On the other hand, many studies have shown that the presence of additives or impurities during the

---

* Corresponding author.
E-mail address: kralj@irb.hr (D. Kralj).

0021-9797/$ – see front matter © 2008 Elsevier Inc. All rights reserved.
doi:10.1016/j.jcis.2008.09.045

precipitation could affect crystal nucleation and/or crystal growth of $CaCO_3$ [16–21].

Up to now, there are no reports on the influence of fatty acid additives on the calcium carbonate production in the semicontinuous carbonation process, during which precipitate of different morphological properties could be produced. In this work, we studied the influence of sodium salt of stearic acid, $CH_3(CH_2)_{16}COOH$, on the precipitation of rhombohedral, scalenohedral and nanosized calcite particles, during the semicontinuous carbonation process. The analytical and technical grade quicklime was used in order to find out the possible impact of naturally occurring impurities on the carbonation and hydrophobization process.

2. Materials and methods

Carbonation process was performed by using either technical grade lime or analytical grade $Ca(OH)_2$. Technical grade CaO was obtained from calcium carbonate raw material, provided by the Kamen Sirač Inc., Croatia. According to chemical analysis, major components of lime were found to be: CaO (94.66%, w/w), MgO (3.14%, w/w), SiO_2 (0.40%, w/w) and CO_2 (1.80%, w/w). Analytical grade $Ca(OH)_2$ (Merck) contained at least 96% (w/w) $Ca(OH)_2$, while the content of magnesium was below 0.5%, w/w. Sodium stearate, NaSt, was prepared by mixing stearic acid, $CH_3(CH_2)_{16}COOH$, (Kemika, puriss.) and sodium hydroxide at 1:1 molar ratio, in the hot deionized water (80 °C). CaO (100 g) was hydrated in 1.0 dm^3 deionized water during 3 h in order to form slaked lime slurry: the mass ratio of NaSt/CaO varied within the range $0.00 < w_{NaSt} < 0.03$.

During semicontinuous carbonation process [6,9], PCC preparation was performed in a thermostated bench-scale glass reactor of 6.0 dm^3 total volume capacity. The concentration of total dissolved calcium, was maintained apparently constant during each experiment, $2.0\ \text{mmol}\,\text{dm}^{-3} < c_{tot} < 17.0\ \text{mmol}\,\text{dm}^{-3}$, by controlling the electrical conductivity of the reacting mixture, and by dosing previously prepared and thermostated $Ca(OH)_2$ suspension, ($\gamma(Ca(OH)_2) = 132\ \text{g}\,\text{dm}^{-3}$) into the reactor. The electrical conductivity and total dissolved calcium concentration of $Ca(OH)_2$ solution were previously correlated. The concentration of total dissolved calcium was determined by means of an ion chromatography system ICS-1000 (Dionex) fitted with a CS16 Analytical Column. Gas mixture with approximately 20% CO_2/80% N_2 (Messer) was used, simulating the flue gases that are commonly used for industrial PCC preparation. Gas mixture was introduced at a constant flow rate, $Q = 1.0\ \text{dm}^3\,\text{min}^{-1}$, into the reactor through the nozzles on the bottom of baffles. The temperature, $20\,^\circ\text{C} < t < 50\,^\circ\text{C}$, and the stirring rate, $n = 1400\ \text{min}^{-1}$, were kept constant during each experiment. The flow of the $Ca(OH)_2$ suspension was stopped 15 min after starting the experiment, while the gas flow was kept constant until the endpoint of carbonation reaction, indicated by an abrupt drop of conductivity. At the end of each experiment, the precipitate was separated, either by 10 min of centrifugation, $n_c = 4000\ \text{min}^{-1}$, or by filtration through a 0.22 μm membrane filter, depending on the size of particles. The precipitate was rinsed with water and dried at 105 °C for three hours. The mineralogical composition of the solid phase was determined by FT-IR spectroscopy (Mattson, Genesis Series) and by X-ray powder diffraction (Phillips PW1830 with a Cu$K\alpha$ radiation). The average crystallite size (D) of the PCC samples showing pronounced broadening of the diffraction lines were calculated by the XRD line broadening method using the Scherrer formula: $D = \lambda/(\beta\cos\theta)$, where λ is the wavelength of radiation, β is full width at half maximum (FWHM) of the diffraction peak after a correction for instrumental broadening, and θ is the diffraction peak angle. The size and morphology of particles were observed by transmission electron microscopy, TEM (FEI Morgagni 268 D and JEOL JEM-1400), and the specific surface area, s, was determined by the multiple BET method (Micromeritics, Gemini), using nitrogen gas as the adsorbate. Thermogravimetric analysis, TGA, was performed at a heating rate of $10\,^\circ\text{C}\,\text{min}^{-1}$ in an air atmosphere using thermoanalyzer TG-50 (Mettler Toledo). The content of calcium and magnesium ions was determined by means of the ion chromatography system mentioned above. The extent of hydrophobicity of different PCC samples was evaluated by the contact angle method and simple floating test on water. The contact angle was measured on a horizontal surface of a PCC sample compressed in a pellet (400 mg) by using contact angle analyzer OCA 20 (Dataphysics). Floating test measured the ratio of floated product to overall weight of sample after the sample was added to water and stirred vigorously [15].

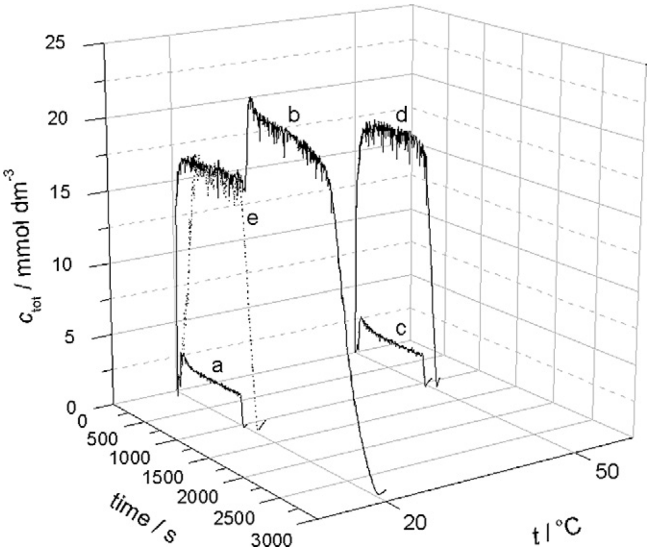

Fig. 1. Typical progress curves of carbonation process performed at $w_{NaSt} = 0.01$ and $t = 20\,^\circ\text{C}$: (a) $c_{tot} = 2.0\ \text{mmol}\,\text{dm}^{-3}$, (b) $c_{tot} = 17.0\ \text{mmol}\,\text{dm}^{-3}$ and $t = 50\,^\circ\text{C}$: (c) $c_{tot} = 2.0\ \text{mmol}\,\text{dm}^{-3}$, (d) $c_{tot} = 17.0\ \text{mmol}\,\text{dm}^{-3}$. Dotted curve (e) represents the carbonation process in which slow addition of lime slurry during the set-point adjustment was applied.

3. Results and discussion

Semicontinuous process of slaked lime carbonation in the presence of NaSt was investigated at different concentration of total dissolved calcium, $c_{tot} = 2.0$, 9.5 and $17.0\ \text{mmol}\,\text{dm}^{-3}$. Fig. 1 shows typical progress curves (c_{tot} vs time) of the semicontinuous process of slaked lime carbonation at different temperatures ($t = 20\,^\circ\text{C}$ and $t = 50\,^\circ\text{C}$) in the systems in which the concentrations of total dissolved calcium were $c_{tot} = 2.0\ \text{mmol}\,\text{dm}^{-3}$ and $c_{tot} = 17.0\ \text{mmol}\,\text{dm}^{-3}$ while the NaSt mass ratio was, $w_{NaSt} = 0.01$. The observed initial increase of c_{tot} corresponds to the $Ca(OH)_2$ dissolution after introduction into the system, while the predetermined constant concentration (concentration plateau) was kept constant by regulating the flow rate of the $Ca(OH)_2$ suspension. The observed fluctuations of c_{tot} from the predetermined value are due to a rather complex precipitation system in which several physical chemical reactions take place in aqueous, solid and gaseous phases, in a reactor of relatively large volume. In spite of a relatively poor regulation at higher c_{tot}, the reproducible production of distinctive morphologies of PCC (rhombohedral, scalenohedral and nanosized calcite) is possible [6–9]. The addition of $Ca(OH)_2$ suspension was stopped 15 min after the onset of the process, while the flow of the gas mixture continued until the excess of $Ca(OH)_2$ was completely carbonated. This part of the process is denoted by a decrease of c_{tot}, and its minimum value indicates the end of the calcium carbonate formation. A subsequent increase of c_{tot} is a consequence of PCC dissolution in the excess of carbonic acid.

The shape of the c_{tot} vs time curve obtained in the experiment carried out at $t = 20\,°C$ and $c_{tot} = 17.0$ mmol dm^{-3} (curve b), differs somewhat from the other experiments, because c_{tot} could have not been fully controlled and kept at the predetermined value. In this system c_{tot} suddenly increases after a period of constancy and the overall carbonation process lasts more than twice longer in comparison to the other runs. This is explained by Carmona et al. [6,22] as a "surface mechanism of precipitation," during which an abrupt dissolution of $Ca(OH)_2$ particles causes an increase of calcium concentration. According to this model, undissolved $Ca(OH)_2$ is initially covered by an amorphous calcium carbonate phase, which nucleates at high initial supersaturation, and which, at certain moment, dissolves and transforms into the stable modification, calcite. Consequently, by exposing the surface to solution, lime starts to dissolve uncontrollably and thus increases the concentration of calcium. However, in our previous work we succeeded to control the conductivity/concentration of total dissolved calcium, even at $t = 20\,°C$ and $c_{tot} = 17.0$ mmol dm^{-3}, by slow addition of $Ca(OH)_2$ suspension during the set-point adjustment at the beginning of the process ($Q_{max}(Ca(OH)_2) = 40$ cm^3 min^{-1}). In this way we have confirmed the decisive role of the excess of suspended $Ca(OH)_2$ in the formation of the precursor phase, amorphous calcium carbonate (ACC), the preparation of particular PCC morphologies and their specific surface areas as well [9]. The respective progress curve of the precipitation system in which a slow addition of the lime slurry, during the set-point adjustment at the beginning of the process, was applied is also shown (curve e). The other experimental conditions in this system ($c_{tot} = 17.0$ mmol dm^{-3}, $t = 20\,°C$) were identical to those in the system in which process went out of control. It should also be emphasized that the shapes of the progress curves and the other properties of the precipitate (morphology, mineralogical composition, size distribution) of the comparable precipitation systems, either containing or without NaSt (not shown), were almost identical.

3.1. Mineralogical composition

Mineralogical composition of the respective PCC samples was determined by both, FT-IR spectroscopy and X-ray diffraction of the powdered samples. Because of the economical reasons and possible large scale PCC production, a particular attention was paid to the properties of PCC prepared by the use of technical grade raw materials, since impurities, particularly Mg^{2+} present in the raw materials (0.83%, w/w), can change morphology, cause the formation of additional polymorphic modifications or incorporate into calcite structure [23,24]. However, the results of X-ray analysis revealed that in all systems investigated in this work calcite was the only crystalline phase obtained at the end of the carbonation process, Fig. S1 in Supporting information.

On the other hand, the FT-IR spectra of the same PCC samples obtained at $t = 20\,°C$, $c_{tot} = 2.0$ mmol dm^{-3} and different stearate content ($0 < w_{NaSt} < 0.030$) exhibited not only the typical absorption bands of calcite, at $\nu_2 = 877$ cm^{-1} and $\nu_4 = 713$ cm^{-1}, assigned as CO_3 out-of-plane deformation mode and OCO bending (in plane deformation) mode, respectively [25], but also absorbencies assigned to stearate alkyl groups (Fig. 2). The absorptions at 2920 cm^{-1} and 2850 cm^{-1}, assigned as asymmetrical and symmetrical C–H stretching vibrations of the stearate alkyl group, confirm the presence of stearate molecules at the calcite surface [5]. In order to estimate the relative amount of stearate adsorbed at the respective calcite samples, the absorption intensities of asymmetrical C–H stretching, $\nu_{as} = 2920$ cm^{-1}, were compared. At that, the intensities were normalized with respect to intensities of calcite absorption band at $\nu_4 = 713$ cm^{-1} (masses of calcite samples were apparently the same: $m_c = 1.50 \pm 0.1$ mg). The measured values continuously increased with increasing w_{NaSt} thus indicating the increase of the amount of stearate adsorbed on the PCC surface (Fig. S2, Supporting information).

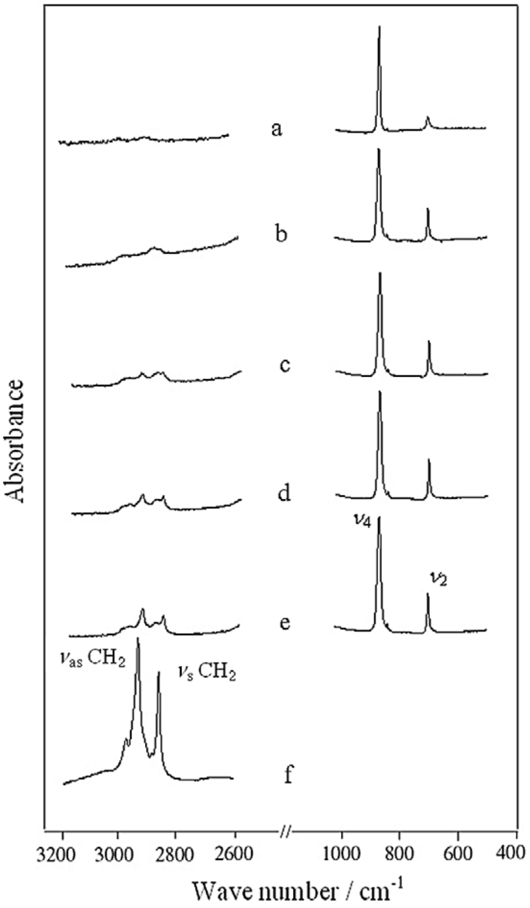

Fig. 2. FT-IR spectra of PCC obtained at $t = 20\,°C$, $c_{tot} = 2.0$ mmol dm^{-3} and different mass ratios w_{NaSt}: (a) 0.000, (b) 0.003, (c) 0.010, (d) 0.020, (e) 0.030. Spectrum (f) corresponds to NaSt.

3.2. Specific surface area

Fig. 3 shows the results obtained from the measurements of specific surface area of the calcite samples prepared from technical grade raw material at $t = 20\,°C$, different concentrations of total dissolved calcium and contents of NaSt. Specific surface areas of calcite, obtained without the presence of NaSt at $c_{tot} = 2.0$ mmol dm^{-3} (Fig. 3a) and $c_{tot} = 17.0$ mmol dm^{-3} (Fig. 3b), were respectively, $s = 1.4$ m^2 g^{-1} and $s = 35.4$ m^2 g^{-1}, indicating that at higher concentration of dissolved calcium the nucleation rate was enhanced and the size of thus produce particles reduced. Addition of NaSt into the both systems clearly increased the surface area of PCC: in the system with $c_{tot} = 17.0$ mmol dm^{-3} the specific surface area increased up to the value $s = 51.0$ m^2 g^{-1}, by increasing the mass ratio w_{NaSt} to 0.01. Further increase of the NaSt content increased the measured surface area just slightly, so that the maximum value of $s = 52.8$ m^2 g^{-1} was reached at $w_{NaSt} = 0.03$. Similar tendency of significant increase of s with increasing NaSt content up to $w_{NaSt} = 0.01$, was observed in the system with lower concentration of dissolved calcium, $c_{tot} = 2.0$ mmol dm^{-3}: the measured specific surface area was $s = 2.5$ m^2 g^{-1}, while the maximum value obtained was, $s = 2.8$ m^2 g^{-1} ($w_{NaSt} = 0.03$).

On the other hand, a slow addition of $Ca(OH)_2$ suspension, $Q_{max}(Ca(OH)_2) = 40$ cm^3 min^{-1}, applied during the set-point adjustment in the system $c_{tot} = 17.0$ mmol dm^{-3} and without the presence of stearate, caused the formation of PCC with a specific

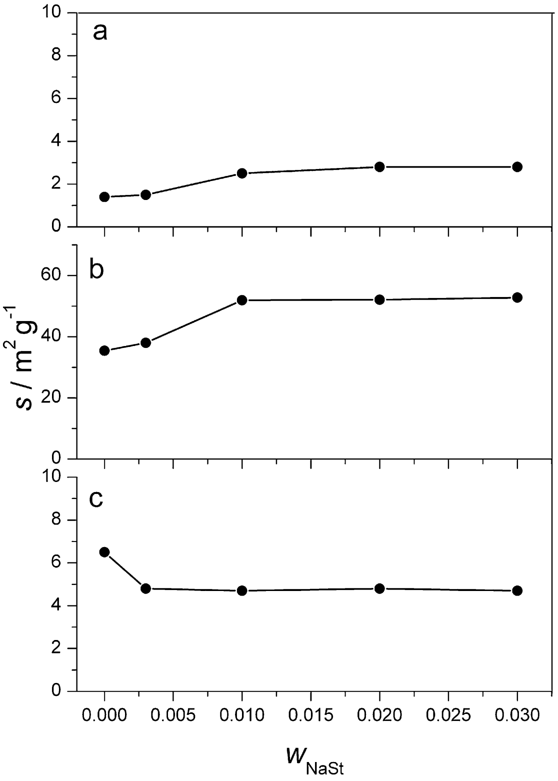

Fig. 3. Values of the specific surface area, s, of PCC samples prepared at $t = 20\,°\mathrm{C}$, different NaSt content and different total dissolved calcium concentration: (a) $c_{\mathrm{tot}} = 2.0\ \mathrm{mmol\,dm^{-3}}$, (b) $c_{\mathrm{tot}} = 17.0\ \mathrm{mmol\,dm^{-3}}$. The system in which $c_{\mathrm{tot}} = 17.0\ \mathrm{mmol\,dm^{-3}}$, but slow addition of $Ca(OH)_2$ suspension during the set-point adjustment was applied ($Q_{\max}(Ca(OH)_2) = 40\ \mathrm{cm^3\,min^{-1}}$) is also shown (c).

surface area $s = 6.5\ \mathrm{m^2\,g^{-1}}$ (Fig. 3c). This is much lower value than that obtained for the PCC produced at uncontrolled conditions. This result indicates that nucleation rate was lower and the average size of thus prepared calcite particles was larger.[1] Opposite to the previously described systems (Figs. 3a, 3b), the addition of NaSt caused the decrease of specific surface area: the value of $s \approx 4.7\ \mathrm{m^2\,g^{-1}}$ was measured for the calcite samples prepared with the addition of all NaSt concentrations applied, $0.003 < w_{\mathrm{NaSt}} < 0.03$.

The addition of NaSt to the system at $t = 50\,°\mathrm{C}$ gave no significant and systematic effect to the specific surface area of PCC and the average values for samples obtained at $c_{\mathrm{tot}} = 2.0\ \mathrm{mmol\,dm^{-3}}$ and $c_{\mathrm{tot}} = 17.0\ \mathrm{mmol\,dm^{-3}}$ were 2.2 and 4.2 $\mathrm{m^2\,g^{-1}}$, respectively.

3.3. Morphology and crystal size distribution

The results of the specific surface area measurements shown above are consistent with TEM observations. Fig. 4 shows the high magnification TEM microphotographs of typical calcite sample prepared under experimental conditions investigated in this work (TEM microphotographs of the same samples, but at lower magnification, are given as Supporting information, Fig. S3). It is evident that in the precipitation systems in which $c_{\mathrm{tot}} = 2.0\ \mathrm{mmol\,dm^{-3}}$, at both temperatures applied $t = 20\,°\mathrm{C}$ and $t = 50\,°\mathrm{C}$, rhombohedral calcite crystals of relatively regular and smooth edges were produced. However, on the addition of stearate ($w_{\mathrm{NaSt}} = 0.02$), the size and the rhombohedral morphology of the crystals were maintained, and just a partial curving of the crystal edges was observed. Similarly, in the precipitation system in which scalenohedral calcite crystals were prepared ($t = 50\,°\mathrm{C}$, $c_{\mathrm{tot}} = 17.0\ \mathrm{mmol\,dm^{-3}}$), the addition of stearate did not significantly change the shape of the crystals.

In the system at $t = 20\,°\mathrm{C}$ and $c_{\mathrm{tot}} = 17.0\ \mathrm{mmol\,dm^{-3}}$, calcite appeared in the form of nanosized, predominantly rhombohedral, particles with the mean particle dimension of $d_{\mathrm{m}} \approx 30$ nm. The average crystallite size calculated by the XRD line broadening method, using the Scherrer formula, was found to be $D = 29.8$ nm ($\lambda = 0.1540598$ nm and FWHM $= 0.3407$ at (104) diffraction peak). The formation of nanosized calcite particles at the given conditions is not surprising, since high concentration of dissolved calcium and low temperature, that permits a higher solubility of CO_2 [22], caused an increase of the driving force for the solid phase formation. Consequently, much higher nucleation rate, in comparison to other systems, and the surface mechanism of precipitation was obtained. It should be mentioned that in spite of the fact that the precipitation process in this system went out of control, the reproducibility of physical chemical properties of the resulting product could have been obtained as long as other process parameters were constant [6,9]. When NaSt was added to this system ($w_{\mathrm{NaSt}} = 0.02$), the rhombohedral shape of calcite particles apparently did not change, but an additional, substantial, fraction of well dispersed particles, with the mean dimension of $d_{\mathrm{m}} \approx 5$ nm, was obtained. The average size of thus prepared calcite crystallites was also estimated by means of the XRD measurements and found to be $D = 24.5$ nm (FWHM $= 0.3849$), thus indicating a decrease in the PCC average crystallite size. This is also consistent with the previously observed significant increase in the specific surface area (Fig. 3b).

The common feature of the above described systems is a production of precipitate that consists of (apparently) distinctive and well defined morphology, either scalenohedral or rhombohedral. However, by changing the process parameters of the semicontinuous carbonation process, the precipitates of some intermediate morphology could be obtained. Thus for example, when slow addition of $Ca(OH)_2$ slurry was applied at the beginning of the process, micrometer sized calcite particles of some intermediate shapes appeared: rhomboscalenohedral crystals were observed in the absence of NaSt, while scalenorhombohedral calcite was obtained in the presence of NaSt [8]. In addition, the presence of NaSt increased the particle size. Calcite precipitated in the system, $c_{\mathrm{tot}} = 9.5\ \mathrm{mmol\,dm^{-3}}$, $t = 20\,°\mathrm{C}$, appeared in the form of spheroidal nanosized particles agglomerated in a chain-like structure. At the same calcium concentration and at higher temperature, $t = 50\,°\mathrm{C}$, much larger calcite crystals, but still not of well defined shape, were obtained; the precipitate could be described as a mixture of rhombohedral and truncated prismatic crystals. Fig. S3 in Supporting information shows the described morphologies.

3.4. Hydrophobicity

Apart from the importance of specific surface area and morphology of PCC, when it is produced for particular purposes, the hydrophobicity of mineral surfaces could be of major significance when PCC is applied as filler in polymer composites. Therefore, the extent of hydrophobicity of the calcite samples, prepared by semicontinuous process, governed at different experimental conditions, was estimated. The so-called floating test was applied or the contact angle between a water droplet and the pellet prepared from respective PCC samples was measured. A particular attention was paid to the study of hydrophobic properties and adsorption of stearate on the calcite samples with well defined shapes, like rhombohedral crystals characterized by the presence of specific {104} crystal faces, and scalenohedral morphology having such {21-1} faces. Rhombohedral {104} surface is the most stable

---

[1] Indeed, in the system in which the precipitation process goes out of the control, the concentration of total dissolved calcium is, at that moment, even higher, $c_{\mathrm{tot}} \approx 22.0\ \mathrm{mmol\,dm^{-3}}$, so the respective nucleation rate is proportionally enhanced.

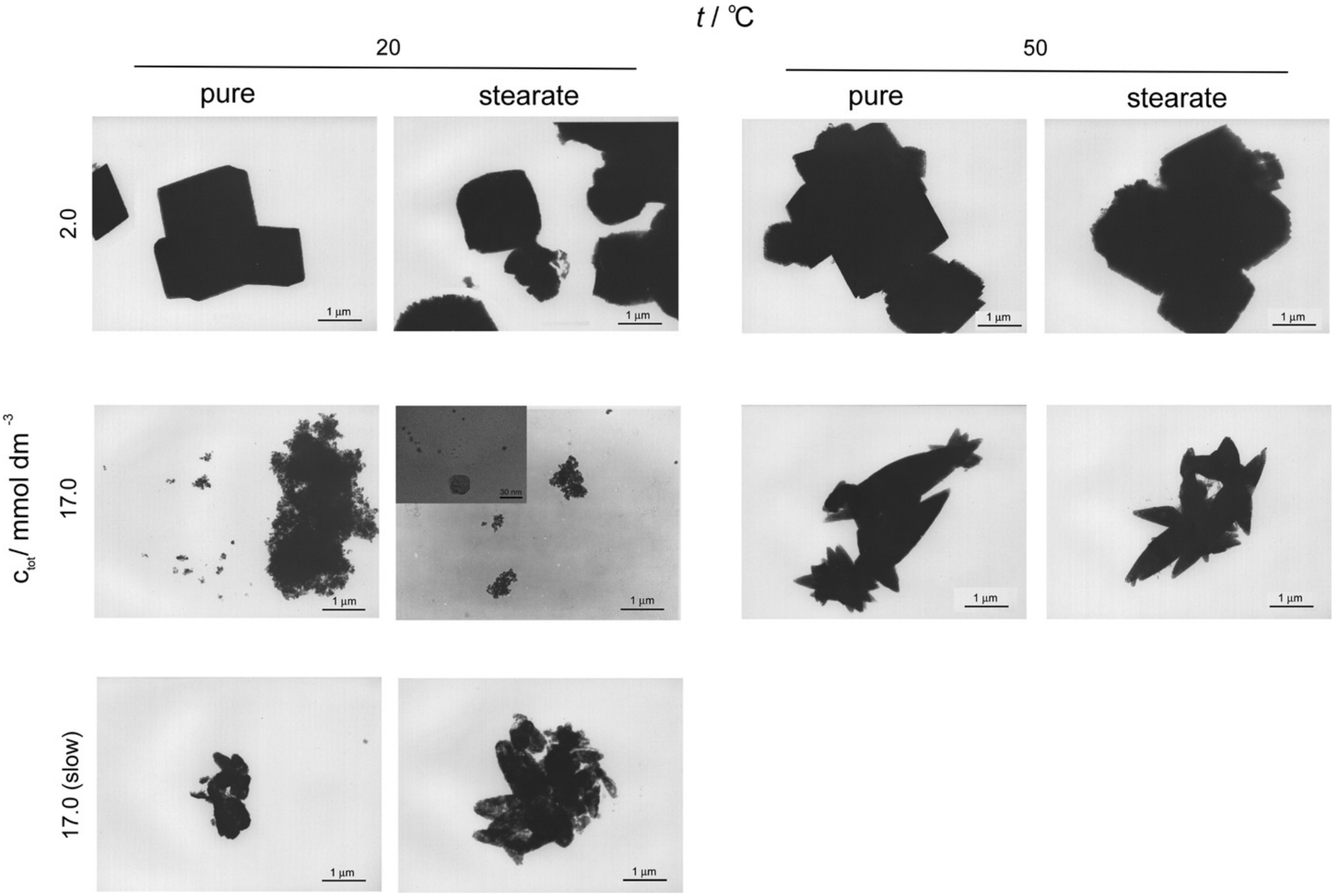

Fig. 4. TEM images of calcite prepared by semicontinuous carbonation process, at different temperatures ($t = 20$ and $50\,^{\circ}\mathrm{C}$) and total dissolved calcium concentration ($c_{\mathrm{tot}} = 2.0$ and $17.0\ \mathrm{mmol\,dm^{-3}}$). Samples prepared by carbonation process in which slow addition of lime slurry during the set-point adjustment was applied ($c_{\mathrm{tot}} = 17.0\ \mathrm{mmol\,dm^{-3}}$ (slow)), without NaSt (pure) and with NaSt at $w_{\mathrm{NaSt}} = 0.02$, are also shown.

among the calcite surfaces and contains equimolar amounts of calcium and carbonate groups, while {21-1} surface is less stable as a consequence of nonstoichiometric content of Ca and CO_3 groups.

Results of the contact angle measurements are summarized and shown graphically in Fig. 5. Contact angles are represented as a function of the mass ratio, w_{NaSt}, for the samples prepared at different temperatures and concentrations of total dissolved calcium. Hydrophobic calcite samples were arbitrary chosen to be those with contact angle $\alpha > 90^{\circ}$. Such samples were obtained at $t = 50\,^{\circ}\mathrm{C}$ and $c_{\mathrm{tot}} = 2.0$ and $17.0\ \mathrm{mmol\,dm^{-3}}$, as well as at $t = 20\,^{\circ}\mathrm{C}$ and $c_{\mathrm{tot}} = 2.0\ \mathrm{mmol\,dm^{-3}}$, in the systems in which the mass ratios w_{NaSt} were above 0.01 (typical images of the contact angle measurements are shown as Supporting information, Fig. S4). Further increase of the content of stearate, up to $w_{\mathrm{NaSt}} = 0.03$, slowly increased the value of contact angle, so that the maximum of about $\alpha = 130^{\circ}$ was obtained for a given set of experimental conditions. In the systems in which calcite was prepared at $t = 20\,^{\circ}\mathrm{C}$ and $c_{\mathrm{tot}} = 17.0\ \mathrm{mmol\,dm^{-3}}$, but at slow addition rate of $Ca(OH)_2$ at the beginning of the process, hydrophobic surface was formed only when the mass ratio w_{NaSt} was above 0.02. This finding can be explained by considering the fact that the specific surface area of thus obtained PCC was higher ($s = 4.75\ \mathrm{m^2\,g^{-1}}$) in comparison to PCC obtained at $c_{\mathrm{tot}} = 2.0\ \mathrm{mmol\,dm^{-3}}$ ($s = 2.78\ \mathrm{m^2\,g^{-1}}$), so the higher amount of NaSt was needed to cover the PCC surface completely.

A completely different behavior was observed for the carbonation process carried out at $t = 20\,^{\circ}\mathrm{C}$ and $c_{\mathrm{tot}} = 17.0\ \mathrm{mmol\,dm^{-3}}$. Hydrophobic property of the samples was not obtained even at the highest addition of NaSt applied, $w_{\mathrm{NaSt}} = 0.03$. This is because of an extremely high specific surface area ($s = 52.8\ \mathrm{m^2\,g^{-1}}$) of the nanosized calcite particles obtained. In order to prepare hydrophobic PCC nanoparticles, additional experiments were performed. In these experiments the addition of NaSt was significantly increased ($w_{\mathrm{NaSt}} > 0.22$), so that a complete coverage of the PCC surface with stearate molecules was possible. The contact angle of thus obtained calcite samples was found to be $\alpha = 128.0^{\circ}$. Simple floating test gave similar and consistent results of the hydrophobicity measurements. A floating ratio of 100%, indicating the hydrophobic nature of calcite samples, was found for the samples shown in Fig. 5 and $\alpha > 90^{\circ}$, the mass ratio being $w_{\mathrm{NaSt}} \geqslant 0.01$.

The content of stearate adsorbed on the surfaces of calcite samples was determined by means of thermogravimetric analysis, shown to be an appropriate technique for determining the content of fatty acids and even the mode of their interactions when adsorbed at calcite surfaces [5]. Fig. 6 shows TGA curves of pure calcite samples, prepared without addition of stearate, as well as of the hydrophobic calcite samples of different specific surface area. Calcite obtained in the absence of NaSt shows only decomposition of $CaCO_3$ (weight loss at about $800\,^{\circ}\mathrm{C}$) while the decomposition of hydrophobic calcite samples occurs in two steps. The weight loss at the temperature range of about 230 to $400\,^{\circ}\mathrm{C}$ corresponds to the removal of adsorbed stearate [1,5], while the loss at about $800\,^{\circ}\mathrm{C}$ corresponds to the mineral phase decomposition. The content of stearate increased with increasing the specific surface areas of the calcite samples and the maximum value of $w = 11.7\%$ was

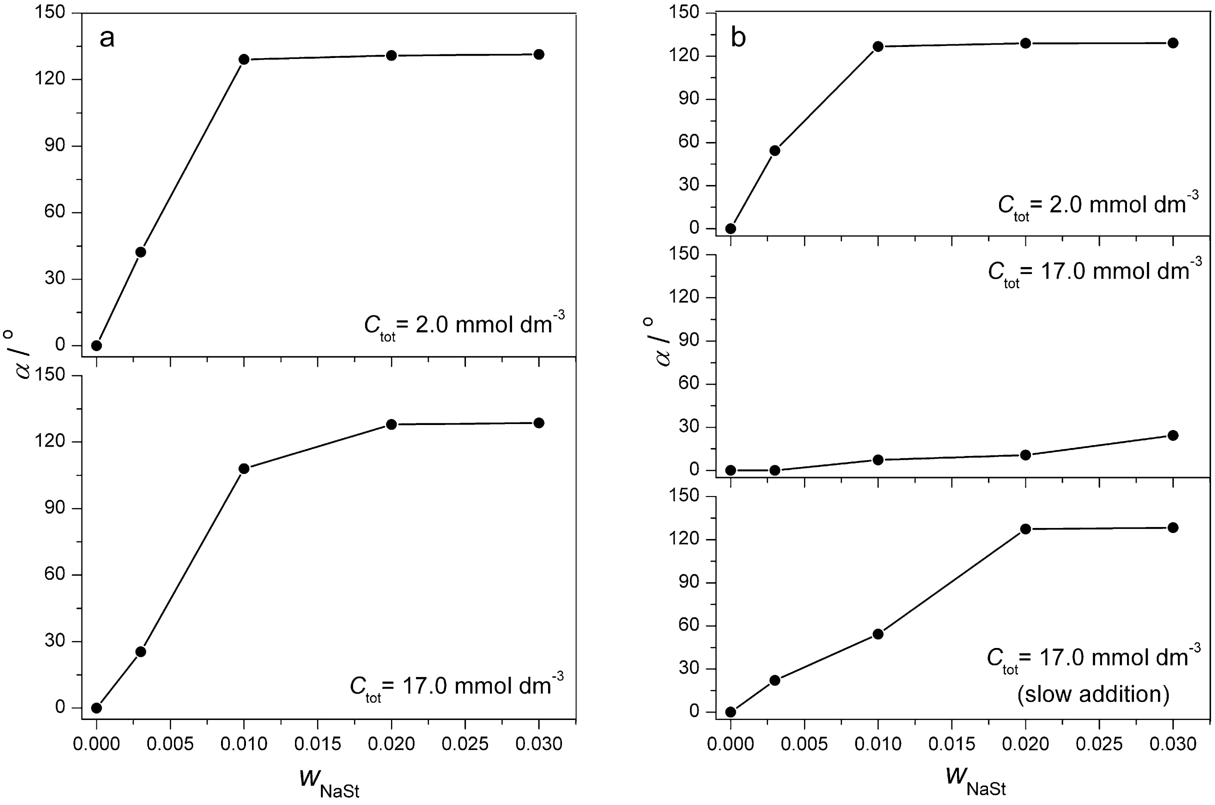

Fig. 5. Plots of the measured contact angle, α, of calcite samples shown as a function of mass ratio, m_{NaSt}/m_{CaO}. The calcite samples were obtained by carbonation process performed at different total calcium concentration, c_{tot}, and temperatures: (a) $t = 50\,^{\circ}C$ and (b) $t = 20\,^{\circ}C$.

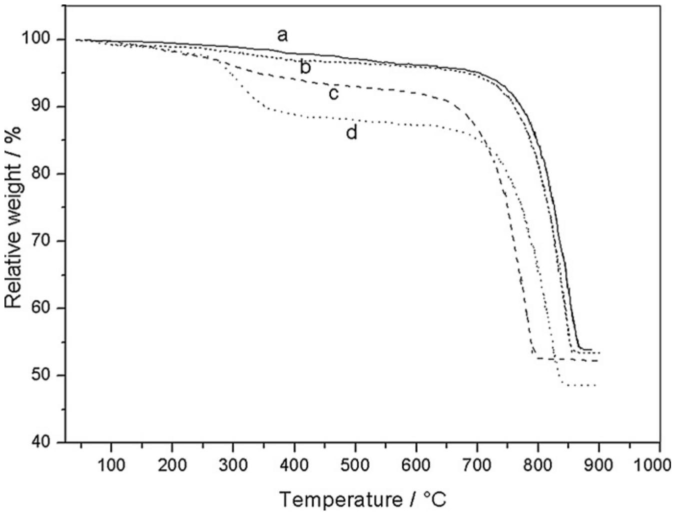

Fig. 6. Thermogravimetric analysis of (a) pure PCC and of hydrophobic PCC samples having different specific surface areas: (b) 2.5 m^2 g^{-1}, (c) 4.2 m^2 g^{-1} and (d) 52.0 m^2 g^{-1}. Samples were obtained, respectively at the addition of the following NaSt mass ratios: $w_{NaSt} = 0.01$, $w_{NaSt} = 0.02$ and $w_{NaSt} = 0.22$.

obtained for nanosized calcite samples with highest surface area of $s = 52.0$ m^2 g^{-1} (curve d).

In order to estimate the extent of calcite surface coverage with stearate monolayer and to compare thus obtained values for different calcite morphologies, the results of the contact angle measurements and the values of the specific surface areas of the respective calcite samples were used [1]. The points represented in Fig. 7, show relationship between the values of the measured contact angles and the calculated surface concentrations of stearate, $\Gamma = n_{NaSt}/A_{PCC}$ (n is the amount of adsorbed stearate and A_{PCC} is the total surface area of calcite), for the samples shown in Fig. 5. The contact angle (hydrophobicity) linearly increases as a consequence of the gradual increase of the amount of stearate adsorbed. Approximately constant value of the contact angle (hydrophobicity) was observed for the higher surface concentrations, which is consequence of two-dimensional aggregation and lateral interactions between hydrophobic alkyl chains of stearate molecules [5]. From the intersection of two straight lines, drawn through the points corresponding to (a) gradual coverage of the surface and (b) the excess adsorption of stearate, the values of surface concentration corresponding to a minimum amount of stearate necessary to build up the monolayer were calculated. In order to prove the concept of site-directed adsorption, the area of one stearate molecule, adsorbed on the morphologically different calcite surfaces, was estimated from the values of minimum surface concentration. The results are summarized in Table 1. For the calcite samples, predominantly consisting of rhombohedral {104} planes with the surface density of 5.05 Ca^{2+} ions/nm^2, the calculated area of one stearate molecule is about 0.21 nm^2. The results are in reason-

Table 1
Estimated values of stearate surface concentration at monolayer coverage, Γ, and calculated cross sectional area of one stearate molecule, a_{St}, of the hydrophobic PCC having different morphologies.

Morphology	Experimental conditions		s	Γ	a_{St}
	t (°C)	C_{tot} (mmol dm^{-3})	(m^2 g^{-1})	(μmol m^{-2})	(nm^2)
Rhombohedral {104}	20	2.0	2.5	7.919	0.210
Rhombohedral {104}	50	2.0	2.2	7.630	0.217
Scalenohedral {21-1}	50	17.0	4.5	5.225	0.317
Nanosized[a]	20	17.0	52.0	6.198	0.268
Scalenorhombohedral {21-1}{104}	20	17.0 (slow)	4.8	7.227	0.230

[a] Probably rhombohedral {104} morphology.

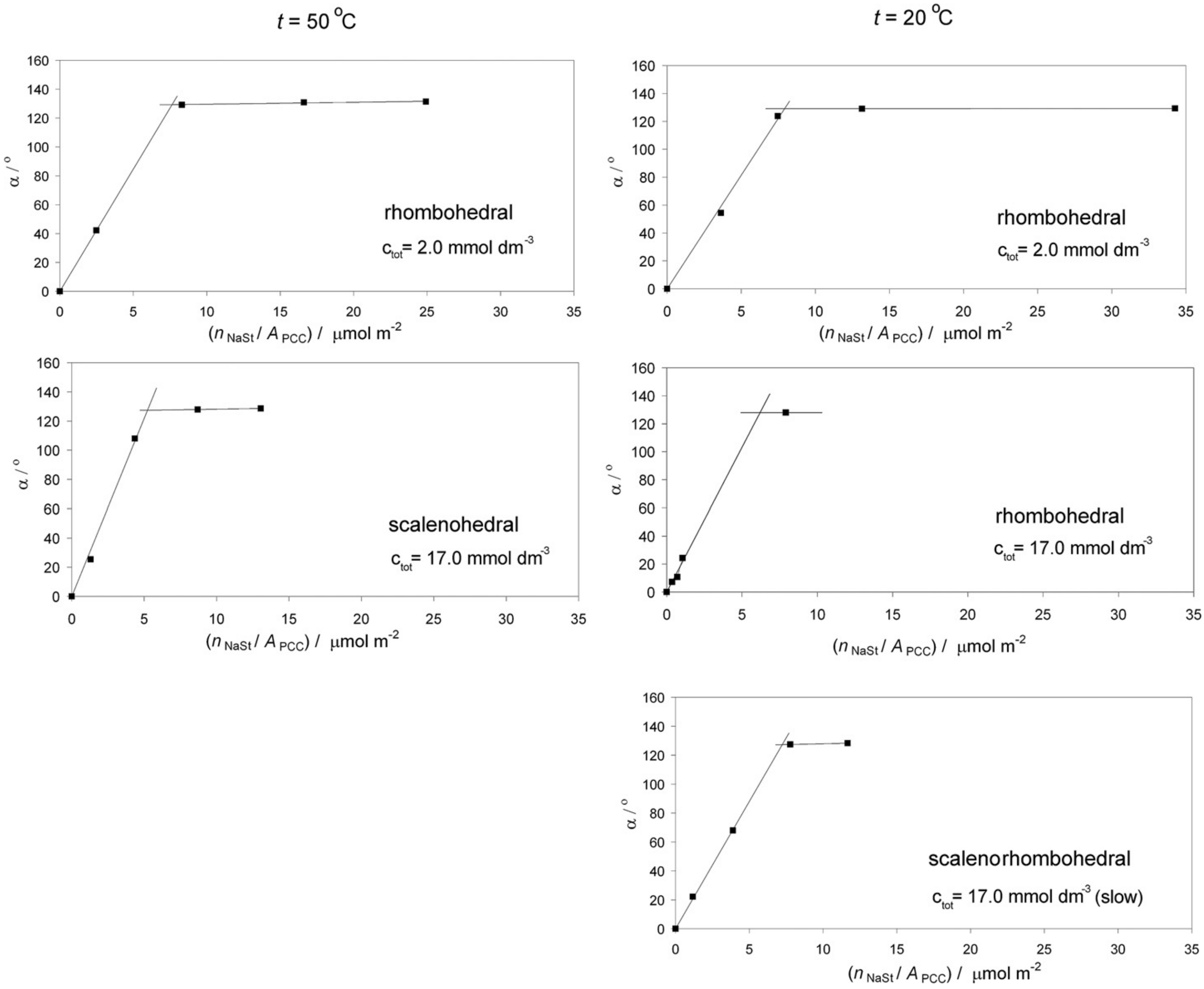

Fig. 7. Plots of the contact angle, α, of calcite samples with different morphologies, shown as a function of stearate surface concentration, $n_{\mathrm{NaSt}}/A_{\mathrm{PCC}}$. Samples were obtained at different temperatures and different total calcium concentrations and correspond to samples shown in Fig. 5.

ably good agreement with the experimentally obtained data for the stearate-treated PCC [1,3–5], and with the data of *in situ* X-ray reflectivity study of stearate adsorption from methanol on Iceland spar calcite crystal, $a_{\mathrm{St}} = 0.199\ \mathrm{nm}^2$ [26]. The model assumes the tilt of alkyl chain of 7% and chemisorption at the surface, through the formation of site-specific bonds between surface calcium ions and oxygen from carboxyl group. It can be described by the reaction:

$$\equiv\mathrm{Ca{-}OH} + \mathrm{HOOC{-}R} \rightarrow \equiv\mathrm{Ca{-}OOC{-}R} + \mathrm{H_2O},$$

where, $\equiv$Ca is the surface calcium ion, and R is the alkyl chain.

The calculated area of one stearate molecule adsorbed on the calcite samples consisting of nonstoichiometric, scalenohedral {21-1} planes,[2] with the surface density of 4.04 Ca^{2+} ions/nm^2, is higher, $a_{\mathrm{St}} = 0.317\ \mathrm{nm}^2$. This result can be explained, either by the lower surface density of Ca^{2+} ions onto which carboxyl group are coordinated and/or by different lateral order of stearate molecules. However, the measured value of $a_{\mathrm{St}} = 0.317\ \mathrm{nm}^2$ is higher than theoretical one, $a_{\mathrm{St}} = 0.248\ \mathrm{nm}^2$, probably just because of lateral disorder and tilting of stearate molecules.

The obtained values for the cross-sectional area of stearate molecules, for intermediate or not well defined calcite morphologies, like rhomboscalenohedral or nanosized calcite, are respectively between the two distinct cases, $a_{\mathrm{St}} = 0.230\ \mathrm{nm}^2$ and $a_{\mathrm{St}} = 0.268\ \mathrm{nm}^2$, which seems to be consistent with the proposed model of stearate adsorption on different calcite faces.

A simplified model of stearate adsorption onto the stoichiometric calcite surface, like {104}, is schematically shown in Fig. 8. The advancement of stearate adsorption (Figs. 8a, 8b) coincide with increasing concentration and corresponds to the linear increase of hydrophobicity (Fig. 7). The attainment of monolayer (Fig. 8c) corresponds to intersection of two straight lines (Fig. 7), while the additional association of stearate molecules (Fig. 8d), resulting from hydrophobic interactions of alkyl chains, does not significantly contribute to the overall hydrophobicity of the precipitate. This is seen as an apparently constant value of the measured contact angle, α (Fig. 7).

---

[2] Actually, {21-1} planes does not cut perfectly calcium ions, so the 0.06 nm slide above and below the plane was considered for calculation of the surface density.

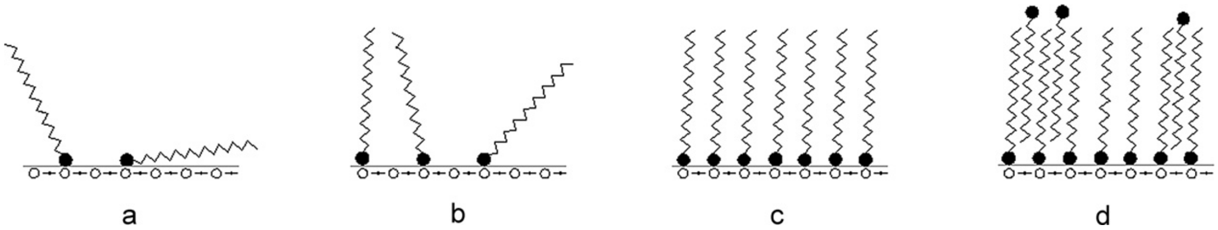

Fig. 8. A simplified model of stearate adsorption onto the stoichiometric calcite surface.

4. Conclusions

The influence of sodium stearate on the precipitation of calcium carbonate, performed in a semicontinuous bench scale reactor, has been investigated. In order to find out optimal conditions for the preparation of PCC with the desired physical–chemical properties (particle size distribution, morphology and hydrophobicity), a range of process parameters, like total dissolved calcium concentration, temperature, initial addition rate of $Ca(OH)_2$ suspension and concentration of NaSt, were varied systematically. It was found that calcite was the only calcium carbonate polymorph that appeared under the investigated experimental conditions, while FT-IR spectroscopy and thermogravimetric analysis of the samples confirmed the presence of stearate on the surface of the precipitated calcium carbonate. The addition of stearate did not significantly change the shape of the calcite crystals, while the specific surface area of rhombohedral and scalenohedral PCC increased with increasing the stearate addition.

It is demonstrated that hydrophobic calcite crystals in the form of rhombohedral, scalenorhombohedral and scalenohedral morphology can be produced at $w_{\mathrm{NaSt}} > 0.01$. The exception is the nanosized PCC production, for which a much higher concentration of NaSt is needed, $w_{\mathrm{NaSt}} = 0.22$.

It was also found that surface concentration, corresponding to the formation of stearate monolayer, is higher for calcite samples predominantly consisting of rhombohedral {104} planes than for calcite samples consisting of nonstoichiometric, scalenohedral {21-1} planes. Lower surface concentration for scalenohedral calcite is explained, either by lower surface density of Ca^{2+} ions of scalenohedral {21-1} planes and/or by different lateral order of stearate molecules.

PCC samples prepared by technical grade quick lime have similar mineralogical and morphological properties as those obtained from analytically pure chemicals.

Acknowledgments

We acknowledge Kamen Sirač Inc., for providing the quicklime, Dr. Sc. Mirela Leskovac for the help with the contact angle analysis and Dr. Sc. Nikola Ljubešić for the TEM analysis. We also thank Dr. Sc. Ljerka Brečević for reading the manuscript and valuable discussions.

This research has been sponsored by the Ministry of Science, Education and Sports of the Republic of Croatia (Project No. 098-0982904-2951).

Supporting information

Supporting information for this article may be found on ScienceDirect, in the online version.

Please visit DOI: 10.1016/j.jcis.2008.09.045.

References

[1] K.A. Rezaei Gomari, R. Denoyel, A.A. Hamouda, J. Colloid Interface Sci. 297 (2006) 470.
[2] Myung-Geun Song, Jomg-Yun Kim, Jong-Duk Kim, Colloids Surf. A 229 (2003) 75.
[3] E. Papirer, J. Schultz, C. Turchi, Eur. Polym. J. 20 (1984) 1155.
[4] E. Fekete, B. Pukanszky, A. Toth, I. Bertoti, J. Colloid Interface Sci. 135 (1990) 200.
[5] M.A. Osman, U.W. Suter, Chem. Mater. 14 (2002) 4408.
[6] J. García-Carmona, J. Gómez-Morales, R. Rodríguez-Clemente, J. Cryst. Growth 249 (2003) 561.
[7] M. Ukrainczyk, J. Kontrec, V. Babić-Ivančić, Lj. Brečević, D. Kralj, Kem. Ind. 56 (2007) 385.
[8] J. García-Carmona, J. Gómez-Morales, R. Rodríguez-Clemente, J. Colloid Interface Sci. 261 (2003) 434.
[9] M. Ukrainczyk, J. Kontrec, V. Babić-Ivančić, Lj. Brečević, D. Kralj, Powder Technol. 171 (2007) 192.
[10] D.K. Keum, K.M. Kim, K. Naka, Y. Chujo, J. Mater. Chem. 12 (2002) 2449.
[11] D.K. Keum, K. Naka, Y. Chujo, J. Cryst. Growth 259 (2003) 411.
[12] C. Wang, Y. Sheng, Hari-Bala, X. Zhao, X. Ma, Z. Wang, Mater. Sci. Eng. C 27 (2007) 42.
[13] C. Wang, P. Xiao, J. Zhao, Y. Liu, Z. Wang, Powder Technol. 170 (2006) 31.
[14] C. Wang, Y. Sheng, X. Zhao, Y. Pan, Hari-Bala, Z. Wang, Mater. Lett. 60 (2006) 854.
[15] Y. Sheng, B. Zhou, C. Wang, X. Zhao, Z. Deng, Z. Wang, Appl. Surf. Sci. 253 (2006) 1983.
[16] J. Kontrec, D. Kralj, Lj. Brečević, G. Falini, S. Fermani, V. Nöthig-Laslo, K. Mirosavljević, Eur. J. Inorg. Chem. (2004) 4579.
[17] J. García-Carmona, J. Gómez-Morales, J. Fraile-Sáinz, R. Rodríquez-Clemente, Powder Technol. 130 (2003) 307.
[18] S. Mann, B.R. Heywood, S. Rayam, J.D. Birchall, Proc. R. Soc. London A 423 (1989) 457.
[19] Y. Sheng, B. Zhou, J. Zhao, N. Tao, K. Yu, Y. Tian, Z. Deng, Z. Wang, J. Colloid Interface Sci. 272 (2004) 326.
[20] N. Wada, K. Kanamura, T. Umegaki, J. Colloid Interface Sci. 233 (2001) 65.
[21] Q. Shen, H. Wei, L. Wang, Y. Zhou, Y. Zhao, Z. Zhang, D. Wang, G. Xu, D. Xu, J. Phys. Chem. B 109 (2005) 18342.
[22] J. García-Carmona, J. Gómez-Morales, J. Fraile-Sáinz, E. Loste, R. Rodríguez-Clemente, J. Cryst. Growth 262 (2004) 479.
[23] G. Falini, S. Fermani, M. Gazzano, A. Ripamonti, Chem. Eur. J. 3 (1997) 1807.
[24] D. Kralj, J. Kontrec, Lj. Brečević, G. Falini, V. Nöthig-Laslo, Chem. Eur. J. 10 (2004) 1647.
[25] F.A. Andersen, Lj. Brečević, Acta Chem. Scand. 45 (1991) 1018.
[26] P. Fenter, N.C. Sturchio, Geochim. Cosmochim. Acta 63 (1999) 3145.